5

# Developments in modelling positive displacement screw machines



Ahmed Kovacevic, Nikola Stosic, Elvedin Mujic and Ian K Smith
*City University London*
*United Kingdom*

## 1. Introduction

It has been estimated that almost 20% of the world's electricity consumption is used for gas compression and pumping. For example, in developed countries, more than 25% of the electrical power output during the summer months is used for the compression of refrigerants in air-conditioning systems.

For most industrial compression and pumping applications, machines of the positive displacement type are used and, due to their technological advantages over other types, approximately 85% of industrial compressors now made, are of the twin screw type. Although these are used for a variety of applications, such as compressors, expanders, blowers, vacuum pumps and liquid and multiphase pumps, the most common use of such machines is for industrial refrigeration, air conditioning and process gas compression.

Depending on the application screw compressors may operate flooded by oil or another fluid or without any form of internal rotor cooling or lubrication. Typical examples of a disassembled oil injected screw compressor and an assembled dry compressor are presented in Fig. 1.

Fig. 1. Typical examples of oil injected and dry screw compressors

The performance of such compressors largely depends on the rotor geometry which may vary, depending on the number of lobes in each rotor, the basic rotor profile and the relative

proportions of each rotor lobe segment. Improvements, to maximise the efficiency, robustness and appearance of these machines are the imperative for every manufacturer in order to be competitive in the market and at the same time to offer a more environmentally friendly product.
Initially, the assumptions on which screw compressors were designed, were that an ideal gas being compressed in a leak proof working chamber by a process, which could reasonably be approximated in terms of pressure-volume changes by the choice of a suitable value of the exponent "n" in the relationship $pV^n$ = Constant.
The advent of digital computing made it possible to model the compression process more accurately and, with the passage of time, ever more detailed models of the internal flow processes have been developed, based on the assumption of one-dimensional non-steady bulk fluid flow and steady one-dimensional leakage flow through the working chamber. By this means and the selection of suitable flow coefficients through the passages, and an equation of state for the working fluid, it was thus possible to develop a set of non-linear differential equations which describe the instantaneous rates of heat and fluid flow and work across the boundaries of the compressor system. These equations can be solved numerically to estimate pressure-volume changes through the suction, compression and delivery stages and hence determine the net torque, power input and fluid flow, together with the isentropic and volumetric efficiencies in a compressor. In addition, the effects of oil injection on performance can be assessed by assuming that any oil passes through the machine as a uniformly distributed spray with an assumed mean droplet diameter.
Such models have been refined by comparing performance predictions, derived from them, with experimentally derived data. A typical result of such modelling is the suite of computer programs described by *Stosic et al, 2005.* Similar work was also carried out by many other authors such as *Fleming and Tang 1998* and *Sauls, 1998.* Due to their speed and relatively accurate results, such mathematical models are often used in industry. However, these neglect some important flow effects that influence compressor performance, mainly in the suction and discharge ports.

## 2. 3D CFD in screw compressors

Screw compressor performance can be estimated more precisely by use of Three-dimensional Computational Fluid Dynamics (CFD) or Computational Continuum Mechanics (CCM).
Computational fluid dynamics (CFD) covers a broad area, which attracted the interest of many investigators at the beginning of the computer era. It is based on the numerical simulation of the conservation laws of mass, momentum and energy, derived for a given quantity of matter or control mass. Three main groups of methods have been developed through the years as described by *Ferziger and Perić, 1995*. The finite volume method is most commonly used in CFD. In the analysis of screw compressors, the aspect of most concern is in unsteady flow calculation with moving boundaries. The usual practice for the analysis of solid body deformation or fluid-structure interaction is by coupling Finite Volume (FV) code with Finite Element (FE) solvers using a specially designed interface. Most CFD and FE vendors use that procedure to take advantages of both FV and FE. Although well established, this procedure in many situations may not be entirely suitable for calculation. One important example of this is that of conjugate heat transfer, where heat transfer in both

the solid and the fluid has to be calculated simultaneously. This is required to estimate the interaction of fluid flow and solid deformation in a screw machine which may be estimated by use of Computational Continuum Mechanics (CCM). In this case, small deformations of solid casing are caused by the large pressure and temperature gradients within the flow domains. Although these deformations are relatively small, they are of the similar order of magnitude as the compressor clearance, and may thus significantly change the flow within the machine, as described by *Kovacevic et all, 2003*.

A number of commercial CFD software packages are currently available which may be able to cope with the complexity of flow through screw machines and may be integrated with CAD. However developed these codes are, there are still limitations in their use for some specific applications. For the analysis of screw machines, a moving, stretching and sliding mesh has to be produced to map the working chamber of a machine. Today's commercial grid generators are still not capable of coping with these demands.

Despite a significant number of papers published in the area of computational fluid dynamics, only a few deal with the application of computational fluid dynamics to screw compressors. All of them are recent papers which started with *Stošić et al* in 1996. That paper describes the principles of three dimensional numerical modelling applied to positive displacement screw machines. However, this work was not fully successful due to the relatively limited grid generation method. *Kovačević, Stošić and Smith* published a number of papers between 1999 and 2001. These papers set up the scene for the commercial use of 3-D numerical analysis in the screw compressor world. In later years, the authors published a series of papers related to both, grid generation in screw compressors and 3D numerical performance estimation, as described by *Kovacevic et al, 2003 and 2005*. These include fluid solid interaction in screw machines, *Kovacevic et al, 2004*.

The breakthrough was made when an analytical transfinite interpolation method with adaptive meshing was used to develop an automatic numerical mapping method for any arbitrary screw compressor geometry. It is explained in detail by *Kovacevic, 2005*. This was later regularly used for the analysis of processes in screw compressors by means of an interface program called SCORG (Screw COmpressor Rotor Geometry Grid generator). This suite enables numerical mapping of both, moving and stationary parts and direct integration with a commercial CFD or CCM code. Although mainly used for CFD in screw machines, the same concept may be used for a variety of other applications. An example of this is the grid generation of the flow paths in a rotary heat exchanger, described by *Alagic et all, 2005*. A recent monograph on CFD in screw machines, by *Kovacevic et al, 2006* gives a comprehensive overview of the methods and tools used. These methods are applicable to all major commercial CFD software packages, capable of coping with complex flows, and can be integrated with variety of CAD systems, as shown by *Kovacevic et al, 2007*.

A typical arrangement of a numerical mesh for CFD calculation of flow in screw compressors is shown in Fig. 2. The moving parts of the flow domain are mapped with a hexahedral block structured mesh while the remaining stationary parts are replaced by the unstructured polyhedral mesh produced by a commercial grid generator directly from the CAD system.

The first experimental verification of numerical results was performed and reported by *Kovacevic et all, 2002*. This study was performed on an oil injected screw compressor with 'N' type rotors with a 5/6 lobe configuration and a 128 mm male rotor outer diameter. The numerical mesh contained a very moderate number of just over half of a million of cells of which around 200,000 were used to map the moving parts of the grid. The converged solution obtained on an office PC was achieved with 120 time steps in approximately 30 hours of computing time. The results were compared with measurements made on the identical screw air compressor. Four piezo-resistive transducers were positioned in the housing to measure pressure fluctuations across the compressor.

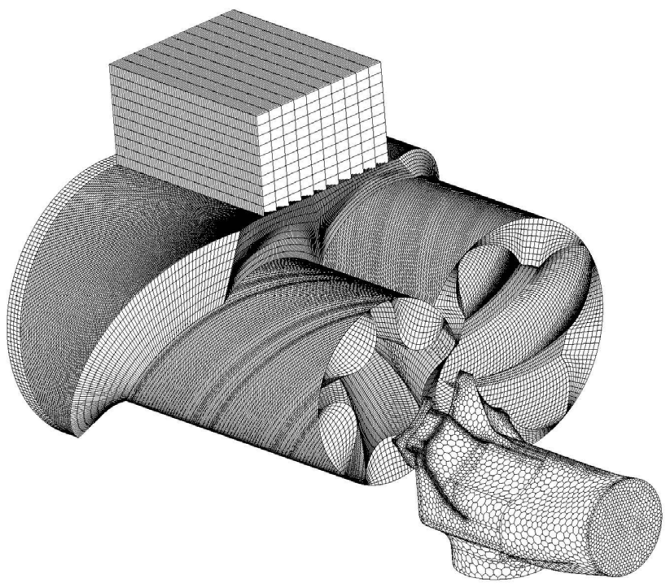

Fig. 2. Numerical mesh for CFD calculation of screw compressor

The results obtained were compared for discharge pressures of 6, 7, 8 and 9 bar respectively. Good agreement was obtained both for the integral parameters and the instantaneous pressure values, as shown in Fig. 3.

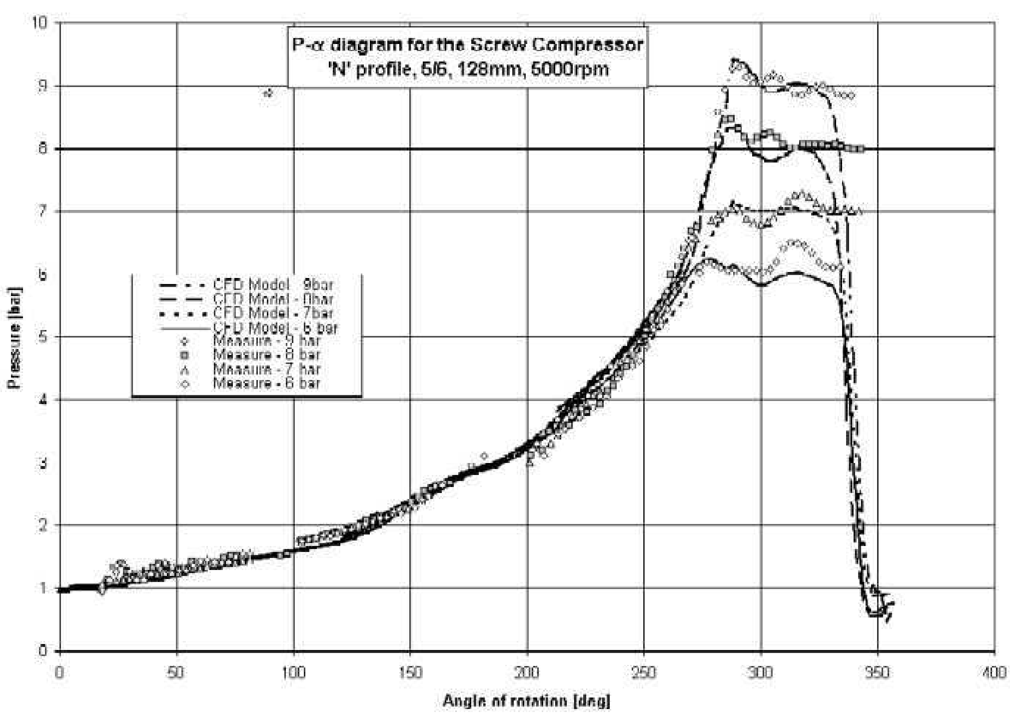


Fig. 3. Comparison of measured and calculated pressures

The report also discussed the effects of various factors on the calculation accuracy. These included variations in mesh sizes, turbulence models, differencing schemes and many other factors. It was concluded that these changes do not affect the overall calculation results which were reasonably accurate and due to that it was recommended that the method can be applied in industry.
However it was also shown that the use of alternative differencing schemes and turbulence methods significantly influence local velocity and pressure values at particular regions of the machine. Although these local values have a low impact on the overall performance, their influence on flow development had to be further investigated. Very few authors have analysed local effects in screw compressors. For example *Vimmr, 2006*, following on *Kauder et al, 2000*, analysed flow through a static mesh of the single leakage flow path at the tip of the male rotor to conclude that rotor relative velocity does not affect flow velocities significantly and that neither of the turbulence models they used significantly change the outcome of modelling. That was in agreement with the findings of *Kovacevic et al , 2006*, but also confirmed that the need for further validation of full 3D CFD results could not be obtained by simplified numerical or experimental analysis. Instead, a full understanding of the local velocities in the suction, compression and discharge chambers of the machine was needed to further validate the existing methods and to develop additional models, if needed.
The following sections include the validation of CFD calculation by the use of Laser Doppler Velocimetry (LDV). Additionally, several examples of the use of CFD for the analysis of different types of screw machines are presented to illustrate the opportunities for the use of CFD both in industry and academia.

### 2.1 LDV flow measurements in a screw compressor

Flow in a screw compressor is complex, three-dimensional and strongly time dependent, similar to that in cylinder flows of gasoline and diesel engines, centrifugal pumps or in turbochargers. This implies that the measuring instrumentation must be robust to withstand the unsteady aerodynamic forces and oil drag, must have a high spatial and temporal resolution and, most importantly, must not disturb the flow. Point optical diagnostics, like Laser Doppler Velocimetry *Durst, 2000, Albrecht et all, 2003, Drain, 1986*, can fulfil these requirements, as described by *Nouri et all, 2006*.
In order to measure flow velocities inside a screw compressor, a test facility was set up at City University, where this technique was used. Extensive measurements were taken of velocities in the compression domain and in the discharge chamber of the test air screw compressor as discussed by *Guerrato et al, 2007*. A transparent window, for optical access into the rotor chamber of the test compressor, was machined from acrylic to the exact internal profile of the rotor casing and was positioned on the pressure side of the compressor near the discharge port, as shown in Fig. 4. After machining, the internal and external surfaces of the window were fully polished to allow optical access. This was obtained to the discharge chamber through a transparent plate, 20 mm thick, installed on the upper part of the exhaust pipe. The optical compressor was then installed in a standard laboratory air compressor test rig, modified to accommodate the transmitting and collecting optics and their traverses, as shown to the right of Fig. 4.
The laser Doppler Velocimeter operated in a dual-beam near backscatter mode. It comprised a 700 mW argon-Ion laser, a diffraction-grating unit, to divide the light beam into two and provide frequency shift, and collimating and focusing lenses to form the control volume. A

Fibre optic cable was used to direct the laser beam from the laser to the transmitting optics, and a mirror was used to direct the beams from the transmitting optics into the compressor through one of the transparent windows.

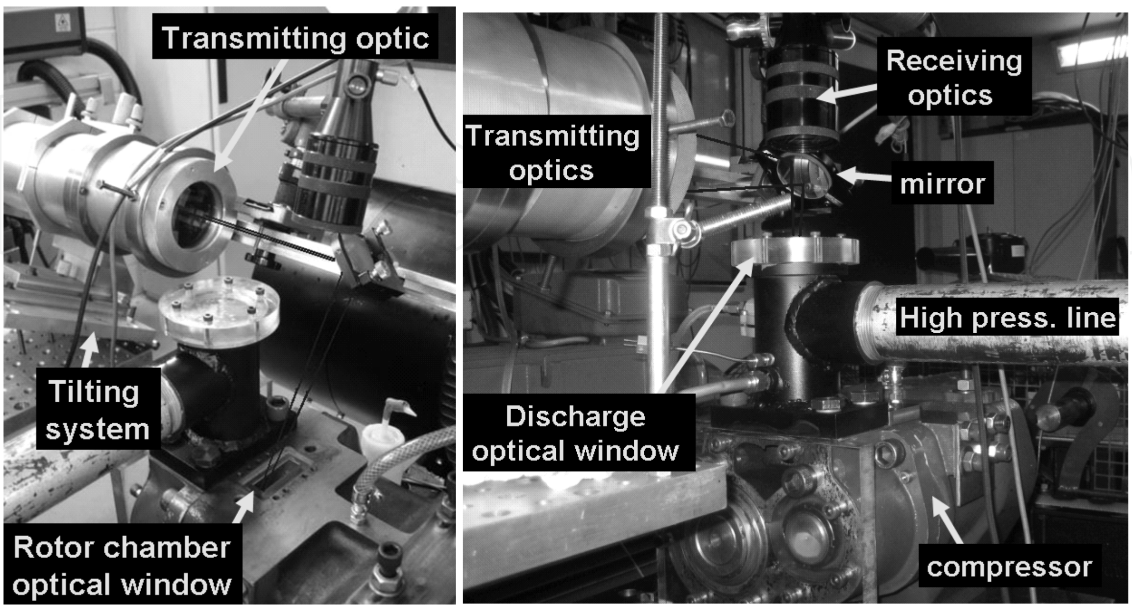

Fig. 4. Optical compressor (left), LDV optical set for discharge chamber (right)

The collecting optics were positioned around 25° of the rotor chamber and 15° of the discharge chamber to the full backscatter position and comprised collimating and focusing lenses, a 100 μm pin hole and a photomultiplier equipped with an amplifier. Although the crossing region of the laser beams is an ellipsoid more than 0.5 mm long, the size of the pinhole defines the effective length of the measuring volume so that it can be represented as a cylinder 100 high and 79 μm in diameter. The fringe spacing is 4.33 μm. The signal from the photomultiplier was processed by a TSI processor interfaced to a PC and led to angle-averaged values of the mean and RMS velocities. In order to synchronise the velocity measurements with respect to the location of the rotors, a shaft encoder that provides one pulse per revolution and 3600 train pulses, with an angular resolution of 0.1°, was used, fixed at the end of the driving shaft. Instantaneous velocity measurements were made over thousands of shaft rotations to provide a sufficient number of samples. In the present study the average sample density was 1350 data per shaft degree. Since the TSI software is provided by 4 external channels, one of them was used to collect the pressure signal coming from the high data rate pressure transducer via an amplifier.

### 2.2 Flow measurements within the compression chamber

Two coordinate systems were defined within the rotor chamber of the compressor, as shown in Fig. 5 (a), (b) and (c). Each of them was applied to one of the rotors where $\alpha_p$ and $R_p$ are, respectively, the angular and radial position of the control volume and $H_p$ is the distance from the discharge port centre. Taking the appropriate coordinate system, measurements were obtained at $R_p$=48, 56, 63.2mm, $\alpha_p$=27° and $H_p$=20 mm for male rotor, and at $R_p$=42, 46, 50 mm, $\alpha_p$=27° and $H_p$=20 for female rotor.
Typical velocity values measured in the working chamber are shown in Fig. 6.

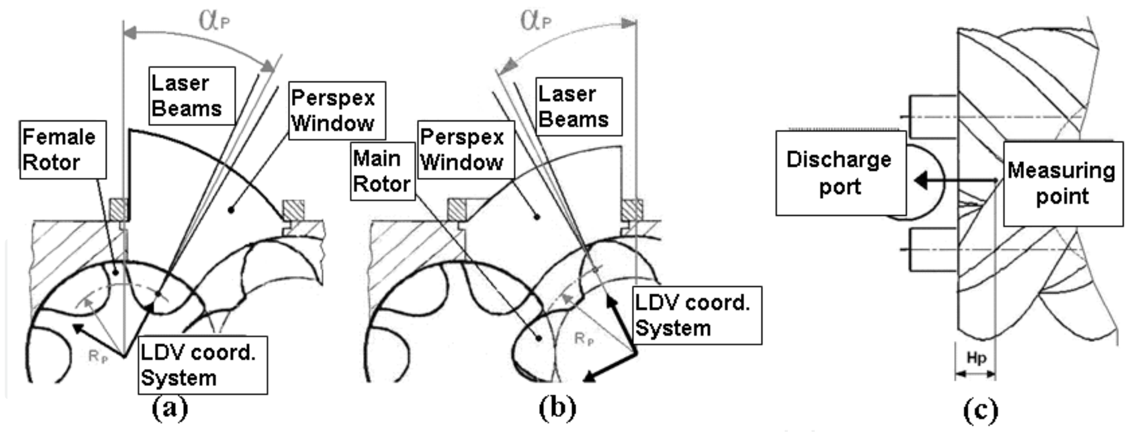


Fig. 5. (a) Coordinate system and window for the female rotor; (b) Coordinate system and window for the male rotor; (c) Axial plane view

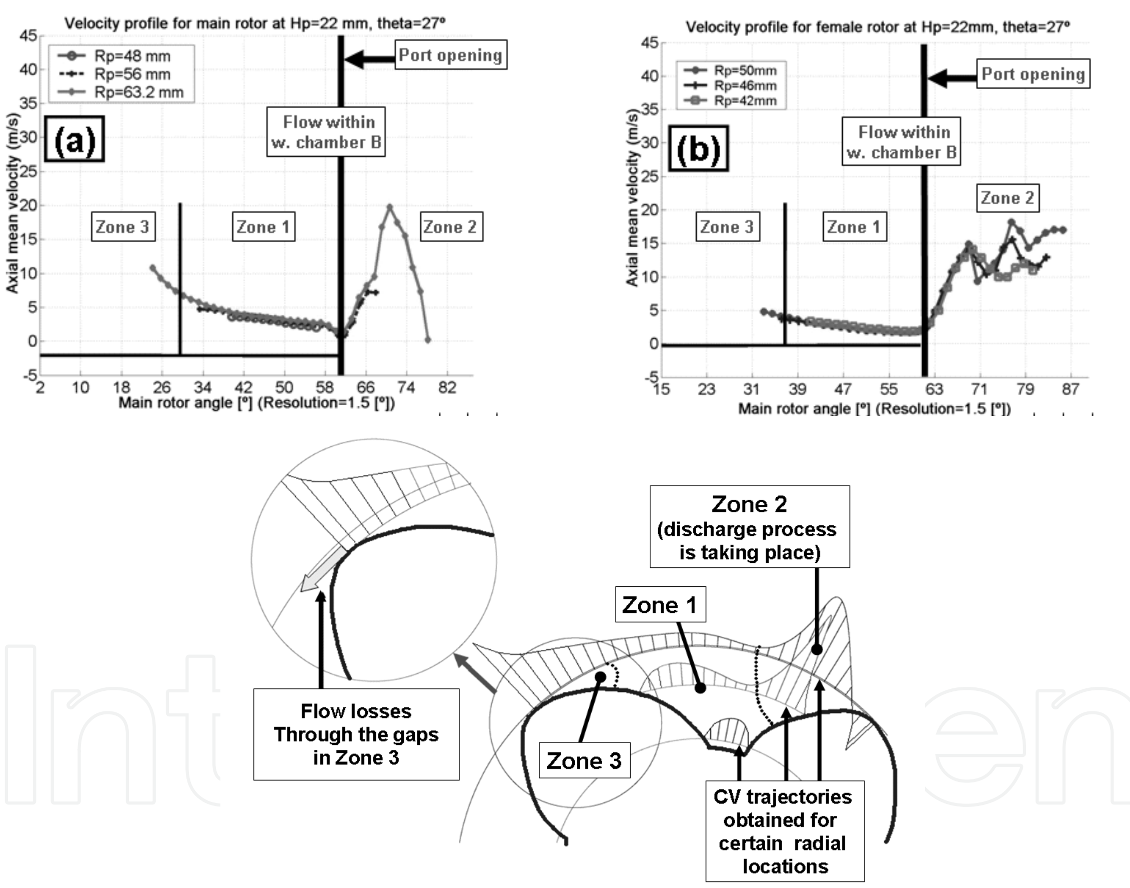


Fig. 6. LDV measurements of the axial velocity in the working chamber (top), Schematic representation of zones in the compressor interlobe domain (bottom)

Three zones were identified in the working chamber near the discharge port. Zone (1) covers most of the main trapped working domain with fairly uniform velocities. Zone (2) is associated with the opening of the discharge port. The velocities and turbulence in this zone are much higher then in Zone (1). In this zone the flow is driven by the pressure difference between the rotors and the discharge chamber. This is especially visible in the case shown,

since the pressure in the discharge system was maintained virtually at atmospheric conditions. Zone (3) is associated with the leakage flows between the rotors and the casing, where velocities increase to values higher then in Zone (1) but are not as chaotic as in Zone (2).
Conclusions derived from the measurements, as explained in more detail in *Gueratto et all, 2007*, are as follows: (1) Chamber-to-chamber velocity variations were up to 10% more pronounced near the leading edge of the rotor. (2) The mean axial flow within the working chamber decreases from the trailing to the leading edge with velocity values up to 1.75 times larger than the rotor surface velocity near the trailing edge region (3). The effect of opening of the discharge port on velocities is significant near the leading edge of the rotors and causes a complex and unstable flow with very steep velocity gradients. The highest impact of the port opening on the flow is experienced near the tip of the rotor, with values decreasing towards the rotor root.

### 2.3 Flow measurements within the discharge chamber

Fig. 7 (a) shows a schematic arrangement of the discharge chamber divided into the discharge port domain and the discharge cavity.
Fig. 7 (b) and (c) show the measurement locations for two characteristic cross sections called the W and V sections. The coordinate system, drawn in all of the sketches in Fig. 7, identifies the location of the measured control volume (CV). Measurements were made at Xp=5.5mm, Zp =13mm and Yp = -8 to 13mm.

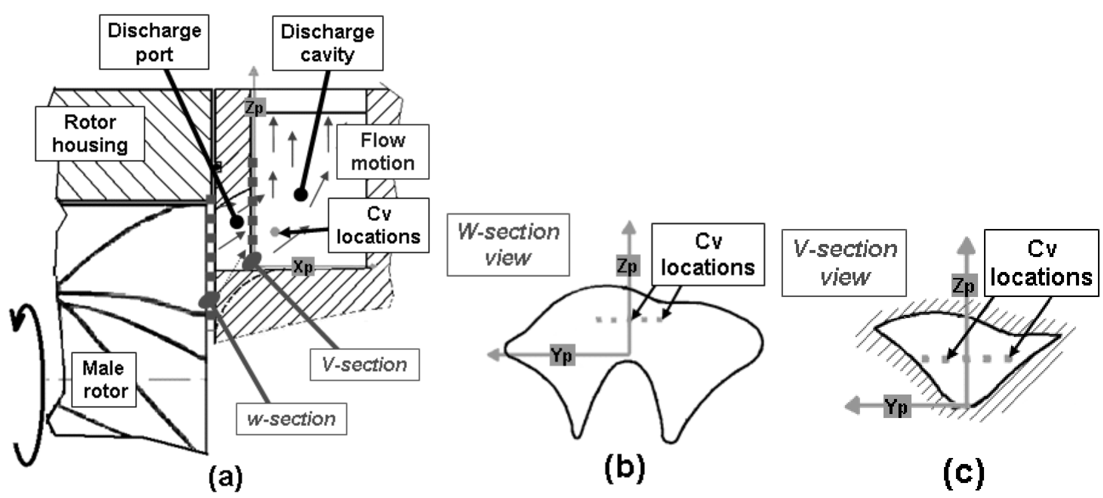


Fig. 7. Measurement points in the discharge chamber: (a) Axial section through the discharge (b) "W" section, (c) "V "section;

Typical measured results in the discharge chamber are shown in Fig. 8. The axial mean flow velocities are obtained using Laser Doppler Velocimetry (LDV) at a rotational speed of 1000 rpm and a pressure ratio of 1.0. The most important findings are as follows. (1) Velocities are higher than in the compression chamber due to fluid expansion in the port between sections W and V. (2) The axial velocity distribution within the discharge chamber is strongly correlated to the rotor angular position since the rotors periodically cover and expose the discharge port through which, at some point, more then one working chamber is connected. The left diagram in Fig. 9 shows the case when only one compression chamber is connected to the discharge port and the flow is relatively stable. This corresponds with the domains to the left of the port opening line in diagrams in Fig. 8. As another chamber with high pressure flow connects to the discharge chamber, in the right diagram in Fig. 9, jet like flows near sides of the discharge chamber passage occur. These are rendered with high velocities in the domain to the right of the thick port opening line in Fig. 8. (3) The jet flows create velocity peaks that make the flow in that region highly turbulent.

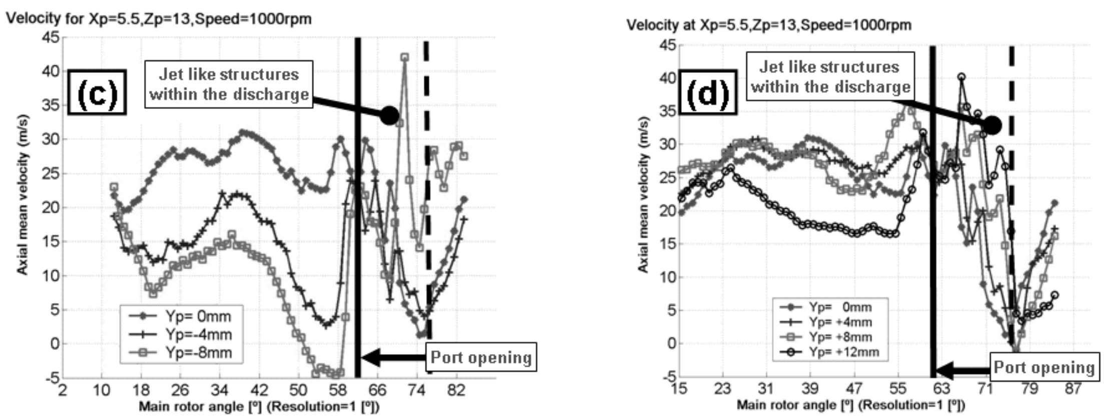


Fig. 8. LDV measured axial velocity component inside the discharge chamber: male rotor side (left), female rotor side (right)

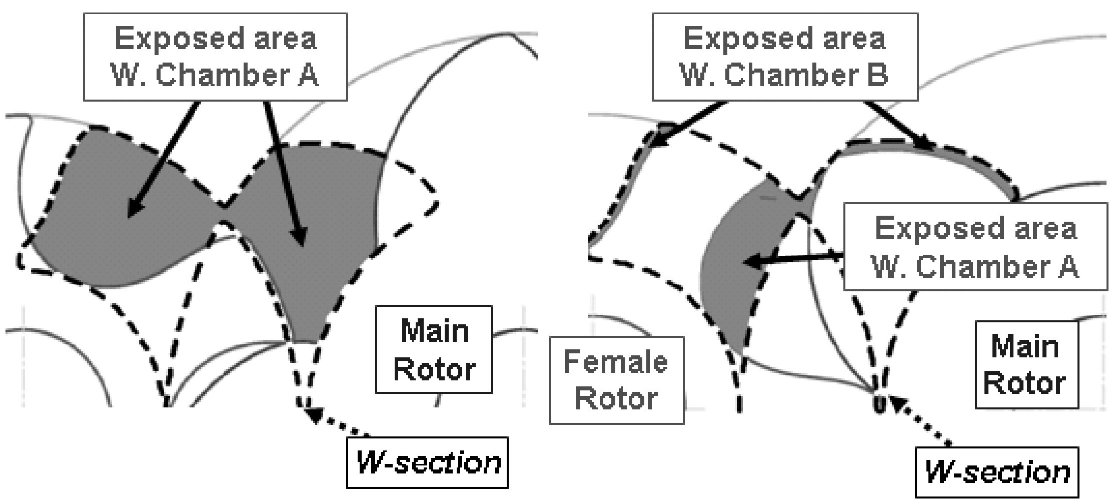


Fig. 9. Schematic view of the periodic exposure of working domains to the discharge port

### 2.4 Validation of CFD results by LDV measurements

The numerical mesh used for CFD calculation and comparison with the measured data, obtained with the LDV technique, is shown in Fig. 2. The flow paths around the rotating parts of the machine are generated using the in-house software SCORG. The pre-processing script generated in SCORG is used to connect these with the stationary numerical mesh of the compressor ports, generated directly from the CAD system, and to transfer the entire case to the CFD solver. Fig. 2 shows the mid sized mesh consisting of 935,000 numerical cells. For the purpose of obtaining a grid independent solution, three different meshes were generated, the smallest consisting of 600,000 numerical cells and the biggest with 2.7 million cells, which was the largest possible case that could be calculated by the single processor of the computer that was used.

### 2.5 Compression Chamber

Due to space limitations, this chapter only compares the CFD results extracted from the middle size model with the LDV results. The compressor working conditions and the position of the CV are identical to the LDV measurements. Fig. 10 shows a comparison of the axial mean velocities in the compression chamber close to the discharge port. This Fig. shows very good agreement throughout Zone (1) and Zone (2), as defined in Fig. 6. In Zone (3) both the measured and calculated velocities increase but the increase in velocities obtained from CFD is larger as a consequence of the inability of the used k-ε model of turbulence to cope with flows near walls in rather large numerical cells. Such a configuration of the numerical mesh is the result of the methodology used for generating and moving the numerical mesh, as explained in more detail by *Guerrato et all, 2007*.

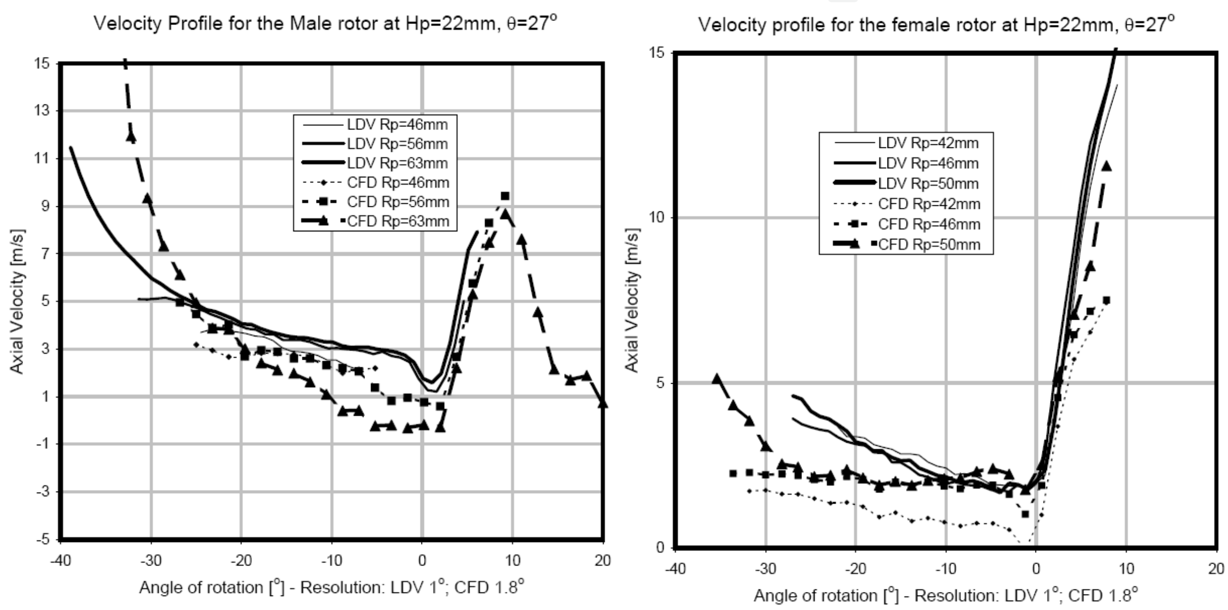


Fig. 10. Comparison of the LDV and CFD axial velocities in the compression domain

### 2.6 Discharge Port

Fig. 11 shows a comparison of the axial velocities in the discharge port. The differences appear to be rather large at locations where the velocities are measured, although the trends and mean values are similar. It is confirmed by calculation that the highest values of the axial velocity are in the middle section through the discharge port, which corresponds to the period of time when only one working chamber is connected to the discharge chamber. On both the male rotor side of the discharge port, as shown in the top diagram of Fig. 11, and on the female rotor side of the port, shown in the bottom diagram, the velocities during that process decrease towards walls. However during the phase when another working chamber is connected to the discharge port, the velocities near the walls increase due to the jet like flows induced by higher pressure differences on the outside of the rotors.

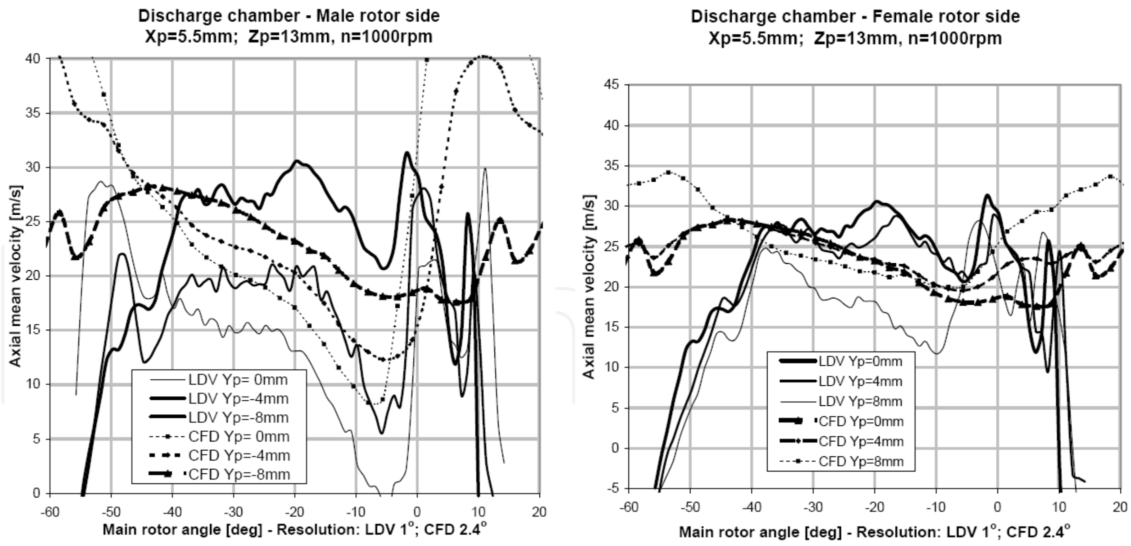


Fig. 11. Comparison of the measured and calculated axial velocities in the discharge chamber

Additionally, leakage flows from the compression chamber to the discharge chamber immediately prior to the opening of the port are large, as shown in Fig. 12. These cause an increase in velocity in the central region of the discharge chamber.

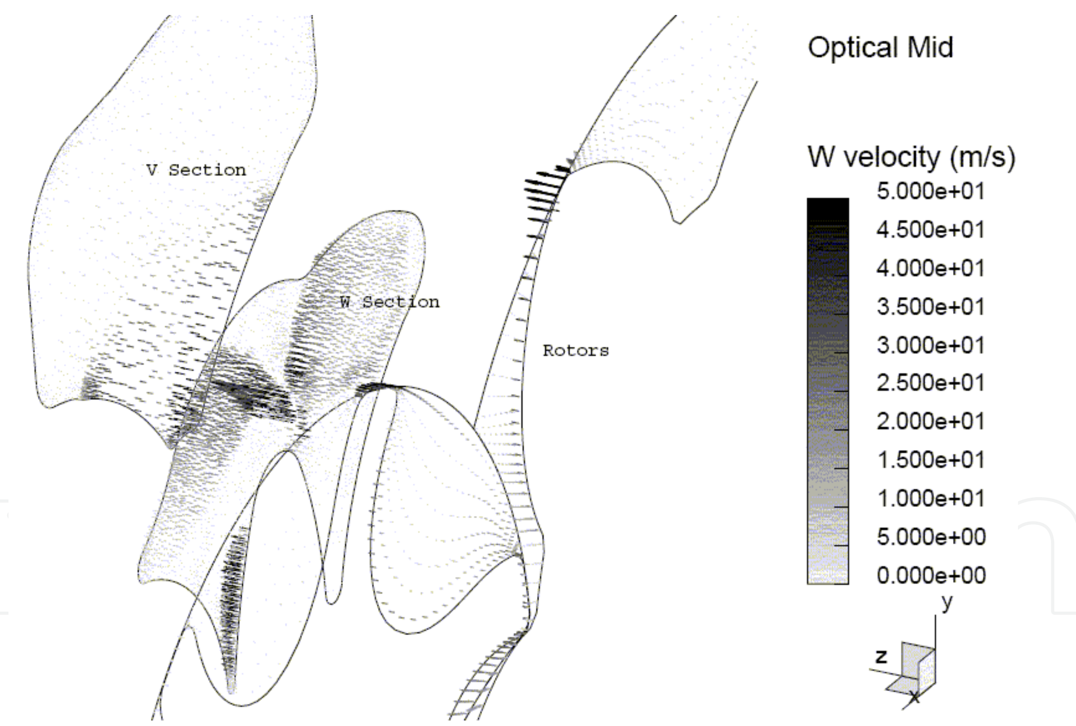


Fig. 12. Axial velocities in three characteristic cross sections in the discharge region of the compressor

The measurements confirm that turbulence plays a significant role in the narrow passage which connects the compression chamber with the large discharge domain. This is most probably the reason why the CFD results do not replicate the measured values more exactly. Therefore further research in the turbulence models for internal flow in the compressor ports is suggested. Favourably, the flow on both sides of that region appears not to be so turbulent. Due to that fact and because the internal energy in positive displacement machines is significantly larger than the kinetic energy, this does not greatly affect the overall estimation of performance. Despite this, further development and improvement of 3D CFD codes are needed.

## 3. Combined Chamber and 3D CFD MODELS

A prerequisite for success in the highly competitive market of screw machines is the ability to design, analyse and produce machines quickly. 3D CFD claculation, although accurate, may take significant time to achieve a desired outcome. Compressor manufacturers are therefore interested in faster but still accurate calculations in order to optimise and improve parts of their machines.

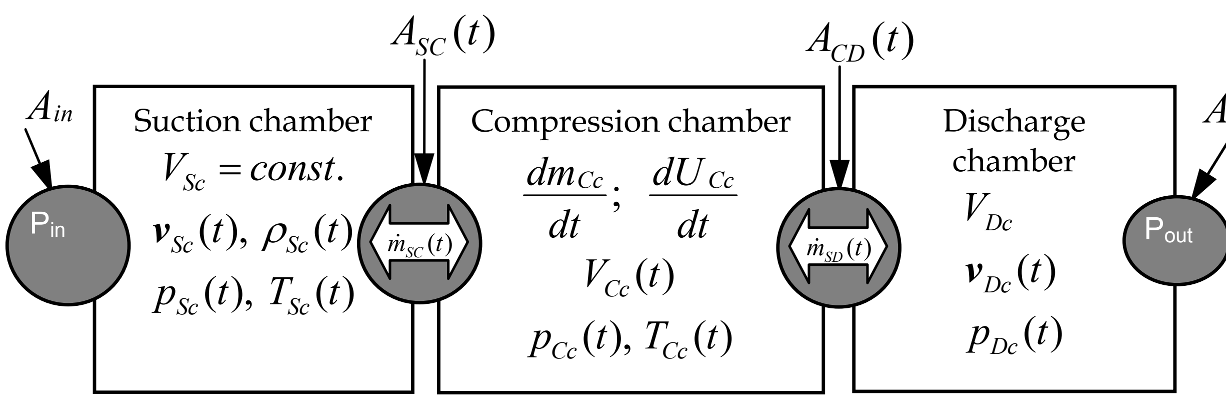

Fig. 13. Schematic representation of a compressor working process

Such a goal can be achieved by use of combined mathematical models in calculation. The idea behind coupled models is that the components of the system of greater interest are modelled with full 3-D simulations while the components of secondary concern are simulated with a thermodynamic model. This can combine the advantages of the fast computation and high flexibility of the chamber model described by *Stosic et all, 2005*, with the enhanced capabilities of the 3-D model, described in detail by *Kovacevic et all, 2006*.
The entire positive displacement compressor can be generally represented by three flow domains which complete a working cycle of the machine. As shown in Fig. 13 the compression chamber in which the compression process occurs is connected to the suction and discharge chambers through which the compressor communicates with the environment. Thermodynamic properties which describe the state of the working fluid in these chambers are namely, the volume of the chamber, the pressure, temperature and the density.
Internal energy changes in positive displacement machines are significantly larger than kinetic energy. In this case the compression process can be quite accurately described by a set of differential equations for internal energy and mass conservation, such as those of *Stosic et al, 2005*. These must be closed with equations that define the leakage flows, liquid injection and heat exchange as well as the mass and energy contributions from the inlet and outlet flows in order to be able to solve them. An equation of state must also be included to establish the relationship of the working fluid thermodynamic properties such as pressure, temperature and volume.

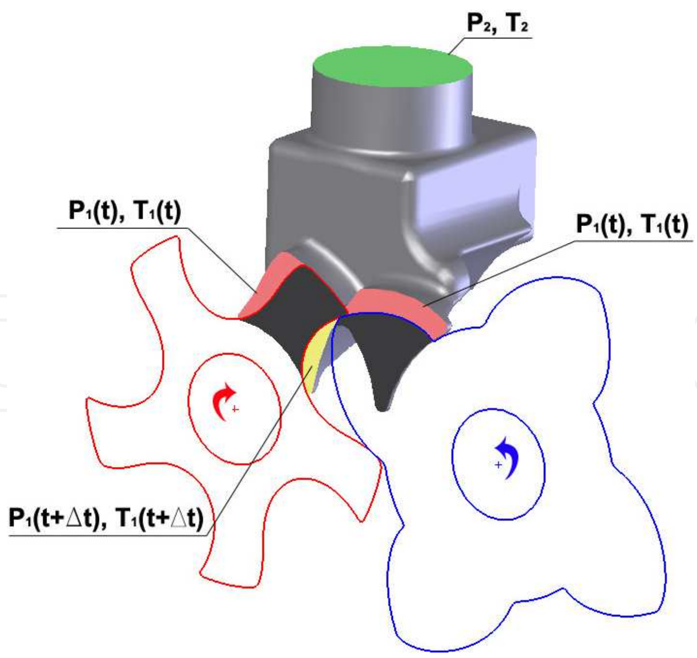


Fig. 14. 3D domain of the screw compressor discharge chamber

The inlet and outlet flows are the means by which a compressor chamber exchanges energy and mass with its surroundings. These occur through openings which generally change both in size and shape with time. More than one of them can be connected to the compression chamber at the same time. In the mathematical models mentioned earlier, these flows are introduced through the enthalpy and mass contributions to the fluid in the compression chamber. If all three chambers are simulated by a quasi one dimensional thermodynamic model, as described by *Stosic et al, 2005*, both the mass and energy flow estimates are based on the assumption of adiabatic flow through the suction and discharge cavities.

However, if a one dimensional model of the compression chamber needs to be integrated with a three dimensional model of the suction and discharge chambers the exchange of mass and energy must be calculated by the summation of the boundary flows that occur in the three dimensional domains. Once the integrated flows are added to those of the one-dimensional model in the compression chamber, they can be used to calculate the thermodynamic properties in that chamber in the form of pressure, temperature and density. The solution of the one dimensional model will then be obtained by integration of the differential equations, typically, using the Runge-Kutta 4$^{th}$ order method, or its equivalent, as described by *Stosic et all, 2005, Mujic et al, 2008 and Mujic, 2009.* The derived values of pressure and temperature in the compression chamber are used later as boundary conditions for the three dimensional models of the suction and discharge chambers. An example of the interface where these boundary conditions are applied is given in Fig. 14.

## 4. CASE STUDIES

### 4.1 Fluid solid interaction

Fluid and solid interaction in screw compressors was investigated for three common applications of screw compressors, namely an oil-injected air compressor of moderate pressure ratio, a dry air compressor, of low pressure ratio, and a high pressure oil flooded compressor. In all cases the rotors are of the 'N' type with a 5/6 lobe configuration.

The rotor deformations in the ordinary oil injected screw compressor are shown in Fig. 15. These cause an increase in the clearance gap between the rotors. However these deformations are of an order of magnitude smaller than the rotor clearances. In order to make the results visible, the deformations in Fig. 15 are enlarged 20,000 times.

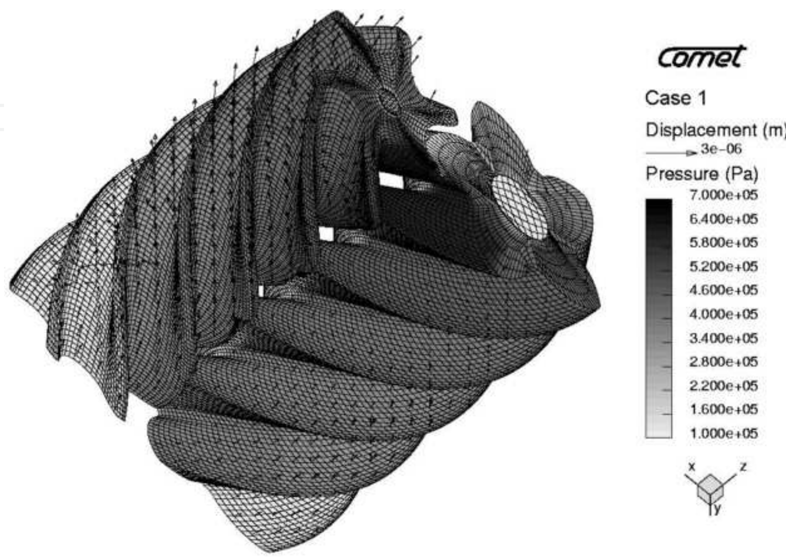


Fig. 15. Rotor deformations in the oil injected compressor

In the oil free air compressor, due to the lack of cooling, the air temperature rise is much higher. For a 3 bar discharge pressure, the exit temperature has an average value of 180$^{o}$C. The deformations of the rotor are presented on the left of Fig. 16. The fluid temperature in the immediate vicinity of the solid boundary changes rapidly, as shown in the right diagram of the same Fig.. However, the temperature of the rotor pair is lower, due to the continuous averaging oscillations of pressure and temperature in the surrounding fluid. This is shown in the right diagram of Fig. 16, where the temperature distribution is given in cross section for both the fluid flow and the rotor body. The deformation, presented in the Fig., is increased 5,000 times in order to make it visible. The rotor deformation has the same order of magnitude as the rotor clearance.

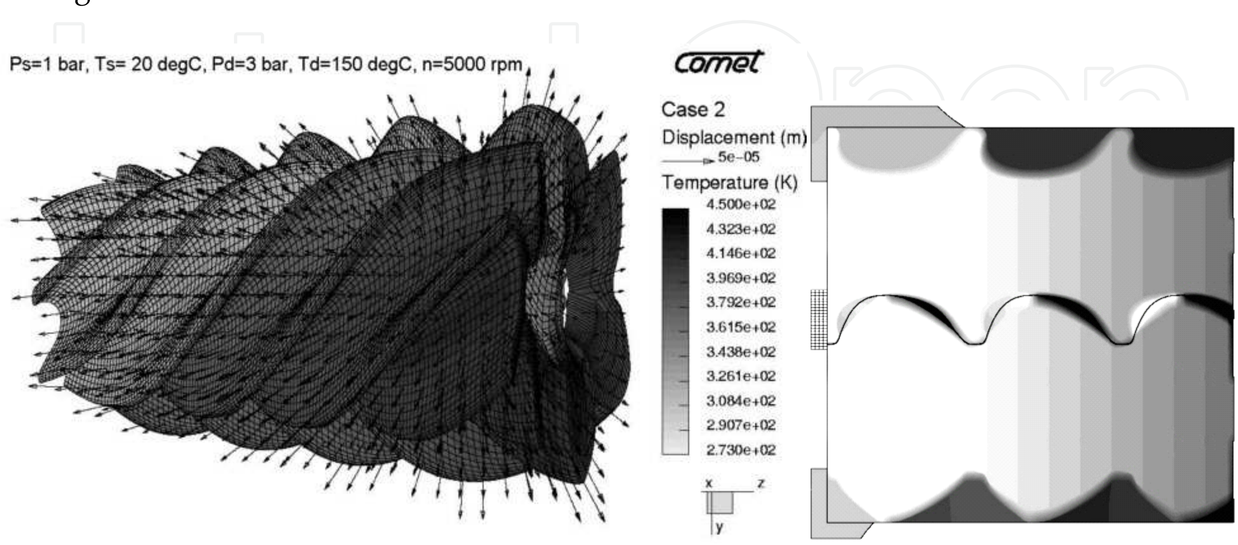


Fig. 16. Rotor displacement vectors and temperature distribution for an oil free compressor

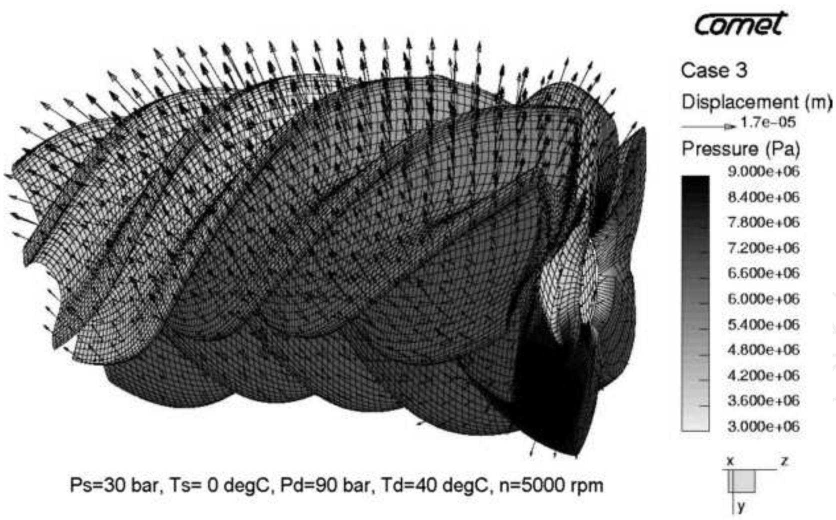


Fig. 17. Deformations of a high pressure oil injected compressor rotors

The high pressure oil injected application was taken as a $CO_2$ refrigeration compressor with suction conditions of 30 bar and 0°C and discharge conditions of 90 bar and 40°C. In this case, the large pressure difference was the main cause of the rotor deflection, with the highest deformation in excess of 15$\mu$m, as shown in Fig. 17. The deformation pattern of the rotors is similar to the low pressure case but with slight enlargement at discharge.

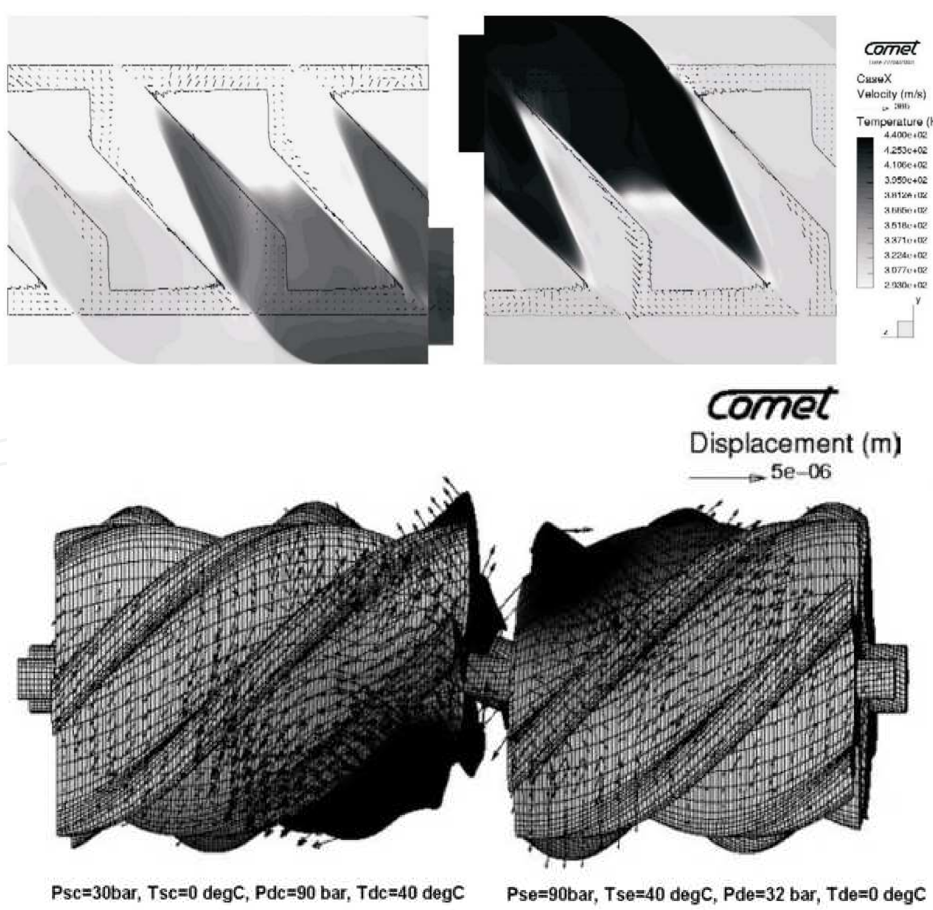


Fig. 18. Deformations of a combined compressor-expander rotors

Fig. 18 shows the temperature distribution and the rotor deformations in a combined compressor-expander for a fuel cell application. The deformation of the rotors is substantially smaller than in the case of the compressor or expander alone. The nature of the deformations suggest that the design of the compressor-expander needs special attention, especially in selecting the rotors and casing materials *Kovacevic et all, 2007.*

### 4.2 Use of CFD for Noise Prediction

Identification of sources of noise in screw compressors and its attenuation becomes an important issue for the majority of applications. Pressure fluctuations in the discharge port affect not only the aero acoustics in that domain but also the mechanically generated noise due to rotor rattling. It is believed that adequate porting can decrease the level of noise and increase the performance of the machine.

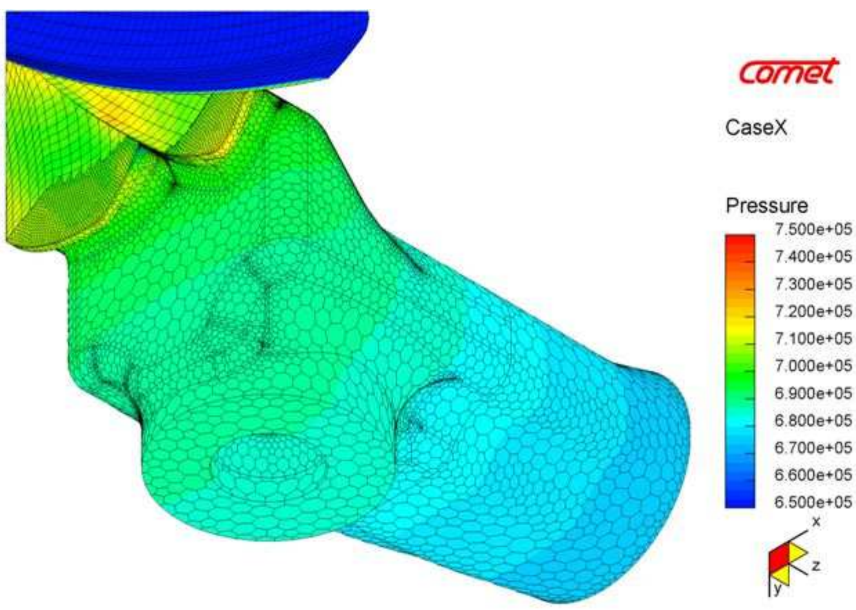


Fig. 19. Pressure oscillations in the 3d CFD model

A chamber model was first used to estimate the pressure oscillations as a function of the shape of the port and the cross sectional area of the connecting flange. These predictions can estimate the main harmonics of generated noise relatively accurately. However, this model does not take into account the shape of the discharge chamber which may play an important role in generating higher harmonics. Further steps were therefore undertaken to analyse pressure fluctuations in the discharge port by a full 3D CFD code. The results obtained by this model agree well with measurements as shown by *Mujic, 2009* but the model is inadequate for everyday industrial use. Therefore a combined model was developed which combines the accuracy of a full 3D model and the speed of a chamber model.
A comparison of the results provided by the three numerical models is shown in Fig. 20.

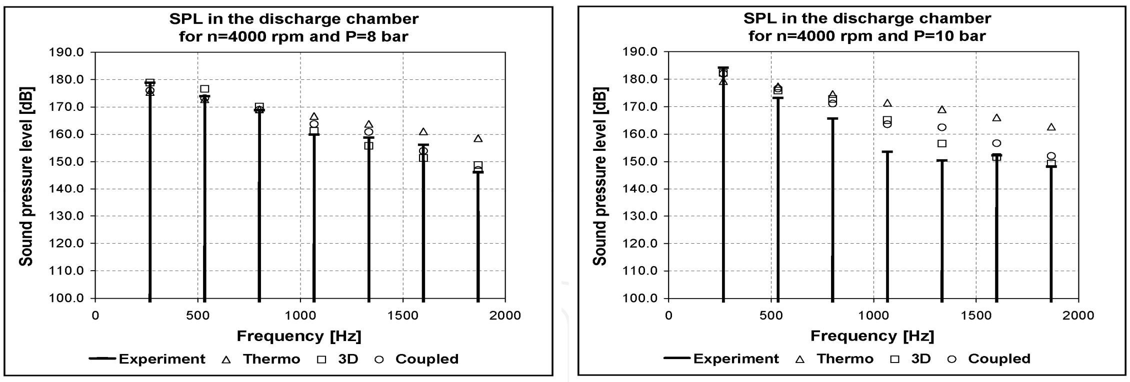


Fig. 20. Comparison of results provided by numerical models

The 3-D and coupled models offer better accuracy than the thermodynamic model, especially for higher harmonics of the gas pulsations. The discharge chamber geometry certainly does influence the gas pulsations and therefore the accuracy of the prediction is thereby improved in the case of the 3-D and coupled models. Additionally, since the thermodynamic model assumes uniform distribution of fluid properties across the control volume the value used for comparison of the results is that obtained at the centre of the discharge chamber. In the case of the 3-D model, the compared pressure values are those taken at the identical position of the pressure probe in the real chamber. As both the 3-D and the coupled models include the momentum equation, they can account for pressure wave propagation through the discharge chamber. The pressure wave passes the measuring place and influences the value of the pressure at that place. Additionally, these two models provide information about other flow properties, such as the velocities within the chamber, and can be useful in the analysis of fluid flow losses.

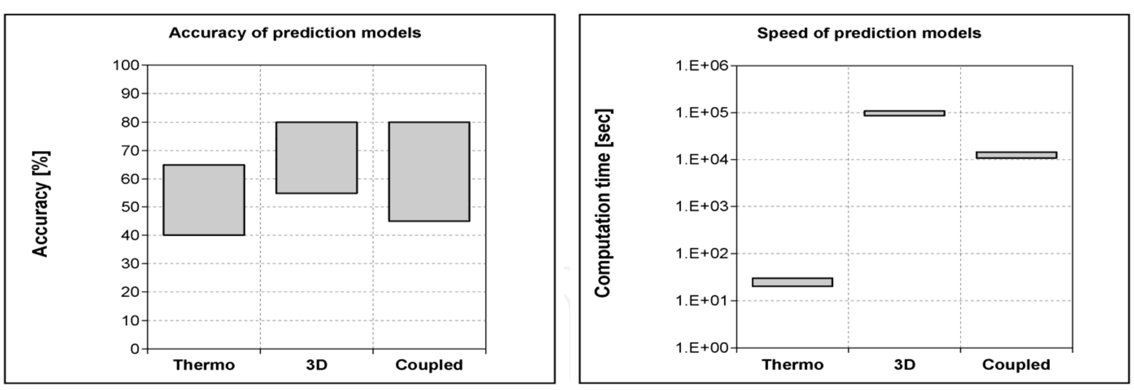


Fig. 21. Accuracy and speed of numerical models

The accuracy and computational time for obtaining a solution with each numerical model are shown in Fig. 21. The chamber model requires modest computer resources and its computational time is much shorter than that required for 3-D computations. The accuracy of the 3-D and coupled models is better than that of the simple chamber model. The coupled model requires one order of magnitude less computational time than the full 3-D model, for negligible loss in accuracy.

### 4.3 Cavitation in gear pumps

The assembly, the functionality and the numerical mesh of a gear pump are presented in Fig. 22. During operation, damage due to cavitation and erosion occurs at the rotor shafts and in the gaps. The work presented here is the property of CFX Berlin. *Steinman, 2006* outlined that the main challenges in this computation were the relatively complex geometry, the relative moving and deforming grids and transient interfaces and cavitation.

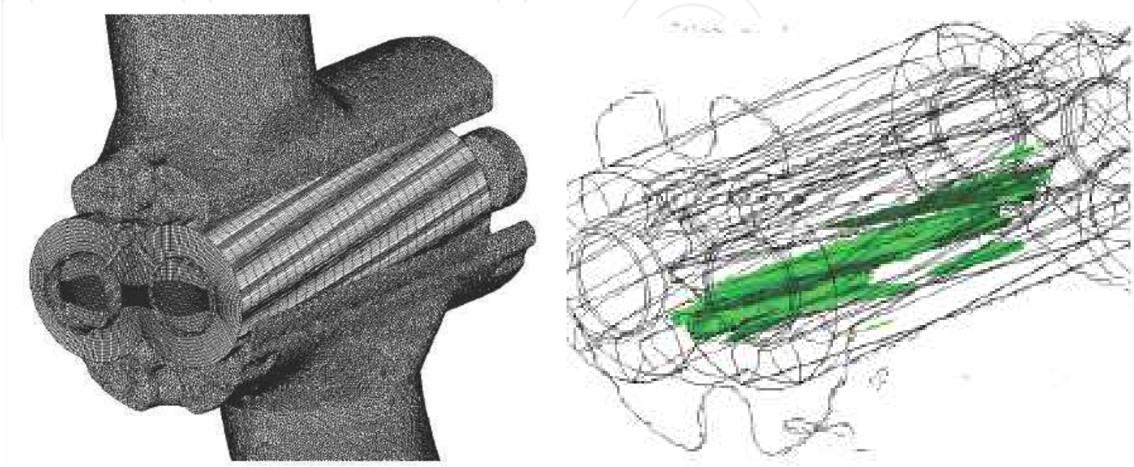

Fig. 22. Numerical mesh of the gear pump and the occurrence of cavitation

The hexahedral numerical mesh of moving parts was generated by SCORG while the stationary parts were meshed by ANSYS CFX and ICEM tools into a tetrahedral mesh. These two domains were connected through transient interfaces (GGI).

### 4.4 CFD analysis of a multiphase screw pump

Multiphase screw pumps are regularly used in the oil and gas industry. The CFD analysis of the leakage flow and pressure distribution in these pumps has been performed by the use of Star CCM+ software. As an example, the pressure distribution on the first layer of cells of multiphase pump passage flow for a 1-10 bar pressure rise is presented in Fig. 23.

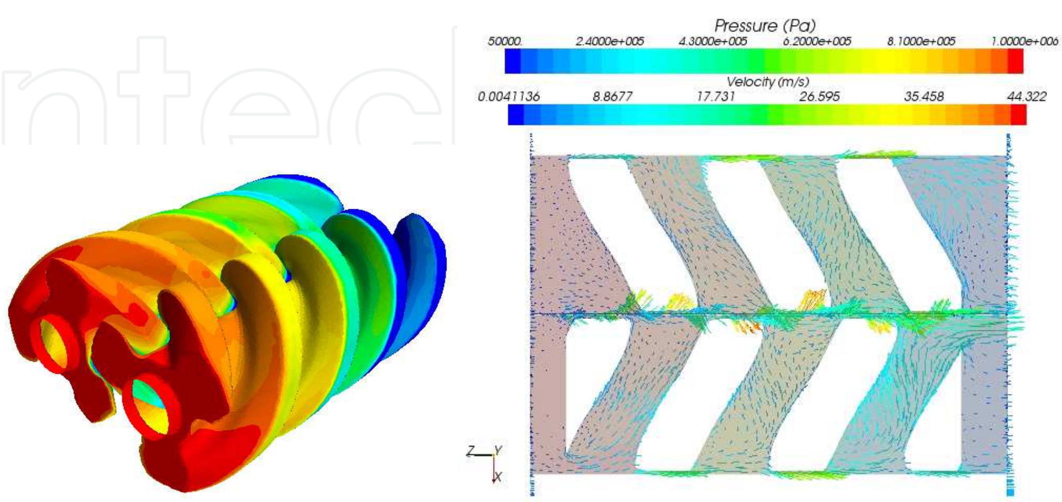


Fig. 23. Pressure distribution on a multiphase oil/natural gas pump and the leakage flow through blow hole area

The leakage flow through the clearances and the blow hole area is shown in the right Fig.23. The numerical grid is obtained by an in-house grid generator originally developed for the analysis of screw compressors. The pressure distribution for alternative multirotor applications is shown in Fig. 24.

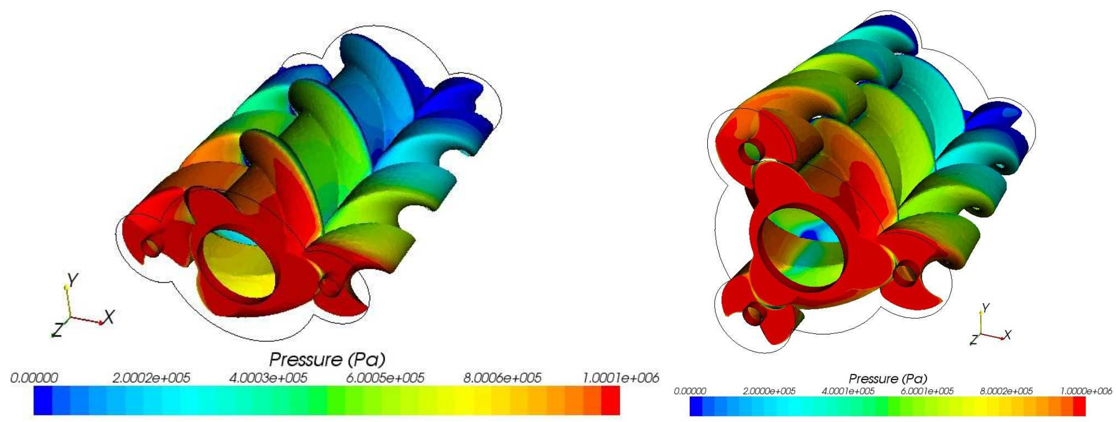


Fig. 24. Pressure field in hydraulic motors with 2 female rotors (left) and three female rotors (right)

As shown in Fig. 24, the machine with three female rotors has a pressure drop between the interlobes that is smaller than in the case of the pump with two female rotors. This allows for smaller leakage flow to be achieved in the machine with more female rotors. However, integration of forces over rotor surfaces gives almost exactly same load on the rotors.

## 5. Conclusions

Various levels of mathematical modelling are used in practice for the performance estimation of screw compressors. Industry mostly uses either empirically fittied or chamber models while researchers tend to use 3D CFD. Extensive study has been performed to validate the accuracy of the 3D CFD results. Laser Dopler Velocimetry (LDV) is used to measure the fluid mean velocity distribution and the corresponding turbulence fluctuations at various cross-sections in the screw compressor. A comparison of measurements and predictions has allowed validation and further development of the CFD package to a stage which will render it possible to design future screw compressors without the need for expensive and time-consuming experiments and 'tuning' of computational models. It appeared evident from LDV measurements that some effects of screw compressor flow are not always well captured by the existing turbulence models. Initial investigation of this problem indicated that a more suitable turbulence model, capable of analyzing flows in the sliding and stretching domains of a screw compressor, may need to be found or developed and validated.

Integrating 3D CFD flow analysis in the suction and discharge chambers with a chamber model in the compression chamber offers the possibility for faster and more accurate analysis when optimising compressor port designs. This is particularly well suited for industrial optimisation. The results obtained are very encouraging but further improvements still may be required.

Four test cases were presented in this publication. They demonstrate the capabilities, accuracy and scope of application of the developed tool.
Mathematical modelling is always a simulation of reality and not reality itself. This publication gives guidelines for the use of existing modelling principles for the performance prediction of screw machines and outlines possibilities for further improvements.

## 6. Acknowledgements

The EPSRC project 'Experimental and Theoretical Investigation of Fluid Flow in Screw Compressors' was performed at City University London between 2006. It was jointly funded by EPSRC, The Trane Company and Lotus Engineering. A part of this paper presents the LDV measurements done by Mr Diego Gueratto for this project. The authors wish to thank all participants in this project for their contribution.
The work on cavitation in gear pumps was performed by CFX Berlin. The authors wish to thank Dr A. Steinman for the permission to refer to it in this paper.

## 7. References

Alagic S., Stosic N., Kovacevic A., Buljubasic I, 2005 *A Numerical Analysis of Heat Transfer and Fluid Flow in Rotary Regenerative Air Pre-Heaters*, Strojniski Vestnik, Journal of Mechanical Engineering, Vol 51, 7-8, pp 411-417, 2005

Albrecht, H.-E., M. Borys, N. Damaschke and C. Tropea, 2003, eds. *Laser Doppler and Phase Doppler Measurement Techniques*. 2003, Springer.

Durst, F., 2000 *Fluid mechanism development and advancements in the 20th century*, in 10th International Symposium on Applications of Laser Techniques to Fluid Mechanics. 2000: Lisbona.

Demirdžić I, Muzaferija S, 1995: *Numerical Method for Coupled Fluid Flow, Heat Transfer and Stress Analysis Using Unstructured Moving Mesh with Cells of Arbitrary Topology*, Comp. Methods Appl. Mech Eng, Vol.125 235-255

Drain, L.E., ed. *The laser Doppler technique*. 1986, John Wiley: New York.

Ferziger J H, Perić, M, 1996: *Computational Methods for Fluid Dynamics*, Springer, Berlin

Fleming J. S, Tang Y, Cook G, 1998: *The Twin Helical Screw Compressor, Part 1:Development, Applications and Competetive Position, Part 2: A Mathematical Model of the Working process*, Proceedings of the IMechEng, Journal of Mechanical Engineering Science, Vol 212, p 369

Guerrato D, Nouri J.M, Stosic N. and Arcoumanis, C. 2007 *Axial flow and pressure characteristics within a double screw compressor*. 3rd Int. Conf. Optical and Laser Diagnostics, ICOLD, 23-25 May 2007, London.

Guerrato D, Nouri J.M, Stosic N., Arcoumanis, C., Smith I.K., 2007a, *Flow Development in the Discharge Chamber of a Screw Compressor*. Int. Conf. on Compressors and their Systems, IMEchE, September 2007, London.

Kauder K., de Araújo-Rudolph L., Sachs R, 2000 *Experimental and numerical investigation of the gas flow using a plane model of male rotor-housing gap in a screw-type machine*. Schraubenmaschinen 8, Dortmund 2000

Kovačević A, Stošić N, Smith I. K, 2003: *Three Dimensional Numerical Analysis of Screw Compressor Performance*, Journal of Computational Methods in Sciences and Engineering, vol. 3, no. 2, pp. 259- 284

Kovačević A, Stošić N, Smith I. K, 2004: *A Numerical Study of Fluid-Solid Interaction in Screw Compressors*, International Journal of Computer Applications in Technology (IJCAT), Vol. 21, No. 4, 2004, pp. 148-158

Kovačević A 2005: *Boundary Adaptation in Grid Generation for CFD Analysis of Screw Compressors*, International Journal for Numerical Methods in Engineering (IJNME), vol. 63, 2005

Kovačević A., Mujic E., Stošić N, Smith I.K, *Clearance Management in Multifunctional Screw Machines*, Proceedings of International Conference on Compressors and their Systems, IMechE London, September 2005

Kovačević A., Stošić N, Smith I.K, 2006: *Screw Compressors Three Dimensional Computational Fluid Dynamics and Solid Fluid Interaction*, ISBN-10: 3-540-36302-5 , Springer Berlin Heidelberg New York

Kovačević A., Mujic E., Stošić N, Smith I.K, *An integrated model for the performance calculation of Screw Machines*, Proceedings of International Conference on Compressors and their Systems, IMechE London, September 2007

Kovačević A., Stošić N, Smith I.K, E. Mujic, 2007, *CFD Integrated Design of Screw Compressors*, Engineering Applications of Computational Fluid Mechanics Vol. 1, No. 2, pp. 96–108

Li, H.F., J.Y. Tu and A. Subic, *The three-dimensional CFD analysis of flow behaviours in a complex twin-screw supercharger*, in The 12th Biennial Computational Techniques and Applications Conference 2004: Melbourne.

Nouri J.M, Guerrato D, Stošić N, Kovačević A, 2006: *Cycle Resolved Velocity Measurements Within a Screw Compressor*, 18th International Compressor Engineering Conference at Purdue, Lafayette, Indiana, USA

Mujic E, Kovacevic A, Stosic N, Smith IK, 2008 *The influence of port shape on gas pulsations in a screw compressor discharge chamber*, Proceedings of the Institution of Mechanical Engineers, Part E, Journal of Process Mechanical Engineering, 2008

Mujic E, 2009 *A Numerical and Experimental Investigation of Pulsation Induced Noise n Screw Compressors*, PhD Thesis, City University London, 2009

Peric M., 2004: *Flow simulation using control volumes of arbitrary polyhedral shape*, ERCOFTAC Bulletin, No. 62, September 2004

Sauls J, 1998: *An Analytical Study of the Effects of Manufacturing on Screw Rotor Profiles and Rotor Pair Clearances*, Proc. VDI Tagung "Schraubenmaschinen 98", Dortmund VDI Berichte 1391

Steinman A, 2006: *Numerical Simulation of Fluid Flow in Screw Machines with Moving Mesh Techniques in ANSYS CFX*," Schraubenmaschinentagung 2006", Dortmund VDI Berichte

Stosic N, 1998: *On Gearing of Helical Screw Compressor Rotors*, Proceedings of IMechEng, Journal of Mechanical Engineering Science, Vol 213 (Part C): p. 587-594.

Stosic N, Smith, I.K. and Kovacevic, A, 2002: *Optimization of Screw Compressor Design, XVI International Compressor Engineering Conference at Purdue*, July 2002

Stošić N, Smith I.K, Kovačević A., 2005: *Screw Compressors Mathematical Modelling and Performance Calculation*, ISBN-10 3-540-24275-9, Springer Berlin Heidelberg New York

Tang Y, Fleming J. S, 1994: *Clearances between the Rotors of Helical Screw Compressors: Their determination*, Optimization and Thermodynamic Consequences, Proceedings of IMechE, Journal of Process Mechanical Engineering, Vol 208, 155

Vimmr J, Ondrey F, 2006, *Numerical Simulation of Leakage Flow Between Moving Rotor and Housing of Screw Compressor*, Proceedings of the Conference Modelowanyie Inzynierskie, ISNN 1896-771X, 32, s. 461-468, Gliwice 2006


**Engineering the Future**

Edited by Laszlo Dudas

ISBN 978-953-307-210-4
Hard cover, 414 pages
**Publisher** Sciyo
**Published online** 02, November, 2010
**Published in print edition** November, 2010

This book pilots the reader into the future. The first three chapters introduce new materials and material processing methods. Then five chapters present innovative new design directions and solutions. The main section of the book contains ten chapters organized around problems and methods of manufacturing and technology, from cutting process optimisation through maintenance and control to the Digital Factory. The last two chapters deal with information and energy, as the foundations of a prospering economy.